Electronic Supplementary Information

Fuel cell-powered microfluidic platform for Lab-on-a-Chip applications

Juan Pablo Esquivel,[a§] Marc Castellarnau,[b,c§] Tobias Senn,[d] Bernd Löchel,[d] Josep Samitier[b,e] and Neus Sabaté*[a]

[a] *Instituto de Microelectrónica de Barcelona, IMB-CNM (CSIC) Campus UAB, 08193, Bellaterra, Barcelona, Spain. Tel:+34 935947700; E-mail: neus.sabate@imb-cnm.csic.es*
[b] *Institute for Bioengineering of Catalonia (IBEC), C/Baldiri Reixac 10-12, 08028 Barcelona, Spain.*
[c] *Current contact information: Research Laboratory of Electronics, Massachusetts Institute of Technology, 77 Massachusetts Avenue, Cambridge, MA 02139, USA; E-mail: mcastell@mit.edu*
[d] *Helmholtz-Zentrum Berlin für Materialien und Energie GmbH, Application Centre for Microenginering, Albert-Einstein-Str. 15, 12489 Berlin, Germany. Tel: + 49 (0) 30 8062 1 5615*
[e] *Department of Electronics, University of Barcelona, C/Martí i Franquès 1, 08028 Barcelona, Spain. Tel: +34 934037181*
§ These two authors contributed equally to this work.

ESI_Table S1. Description of the different stages in the sample flow rate: (i) general description, (iii) transient analysis, and (iii) analysis of the fluidic resistance.

(i) General description

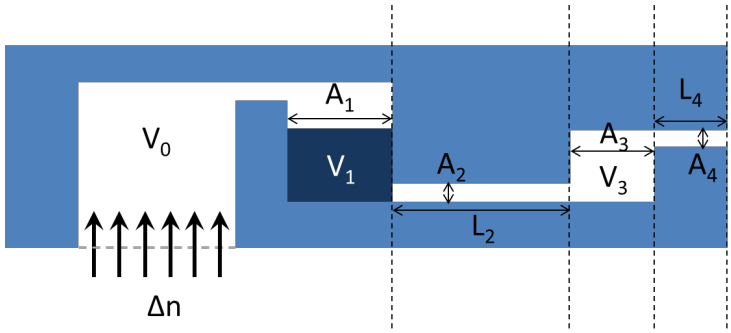

Longitudinal cross-section of the microfluidic device: Δn, moles of CO_2; V_0, initial volume of CO_2; V_1, sample volume; A_1, sample chamber horizontal area; A_2, interconnecting channel vertical area; L_2 interconnecting channel length; V_3, analysis chamber volume; A_3, analysis chamber horizontal area; A_4 exit channel vertical area; L_4, exit channel length.

The following qualitative analysis assumes ideal situation, where CO_2 do not dissolve with the sample, and neither the gas nor the liquid sample produce any deformation on the PDMS channels. Then, for a given fuel cell regime (electric current I), a certain amount Δn of CO_2 will be produced and directly transformed into pressure at the CO_2/sample interface. The pressure drop along the device can be linearly related with the volumetric flow rate through the fluidic resistance. According to those assumptions, then the analysis of the flow rate Q can be described as follows:

- A_1/A_2 and A_2/A_3 determine transients of Q in Region 1 and together with L_2 determine the transient time Δt of Region 1.
- V_3 determines Δt of Region 2.
- A_3/A_4 and A_4 to open space determine transients of Q in Region 3 and together with L_4 determine Δt of Region 3.
- V_1/V_3 determines Δt of Region 4.
- Q in Regions 2 and 4 is mainly determined by A_2 and L_2, as that channel is the major contributor in the total fluidic resistance.

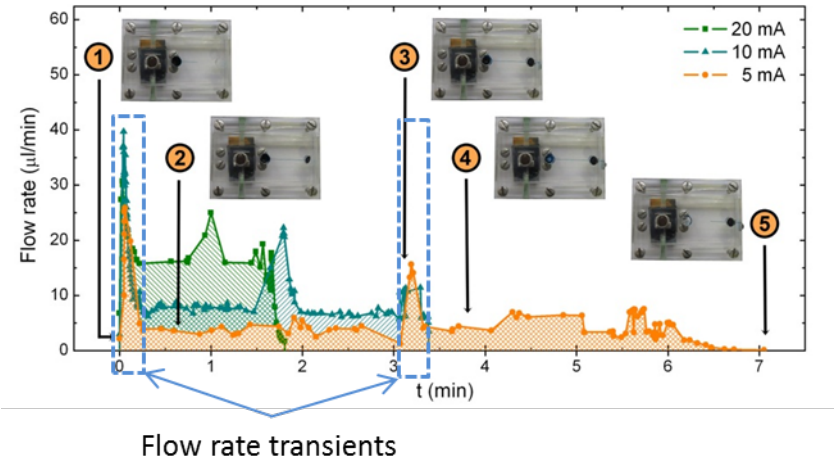

(ii) Transient analysis

Region	Microfluidic component diagram
0	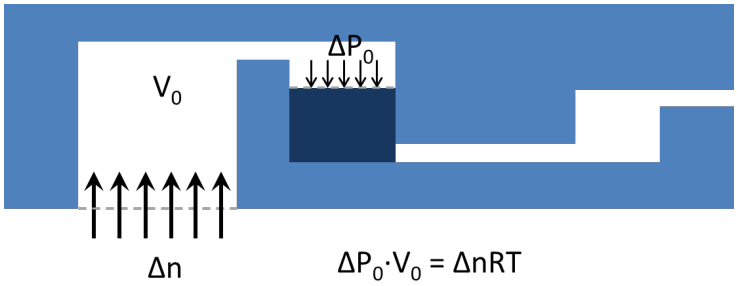 Before the system starts pumping → gas compression @ fixed volume V_0 → pressure increases until the applied force wins surface tension at the outlet of the sample chamber. Pressure at this point determines the initial flow rate in Fig 4, and should be greater than atmospheric pressure.
1	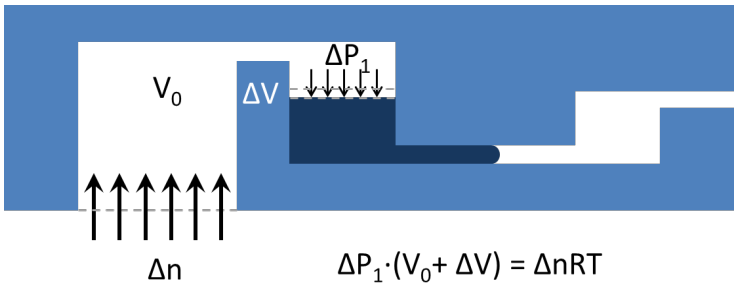 System starts flowing according to the previous situation → the available volume for CO_2 increases (ΔV), but the CO_2 production rate is kept according to the stoichiometric reaction. 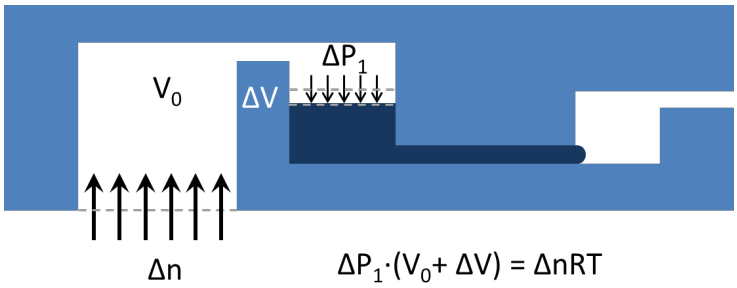 Flow is first accelerated due to the accumulated pressure (ΔP_0) and the cross-section difference between the sample chamber and the main microchannel (A_1/A_2). Then, the flow decreases as soon reaches the analysis chamber (A_2/A_3).
2	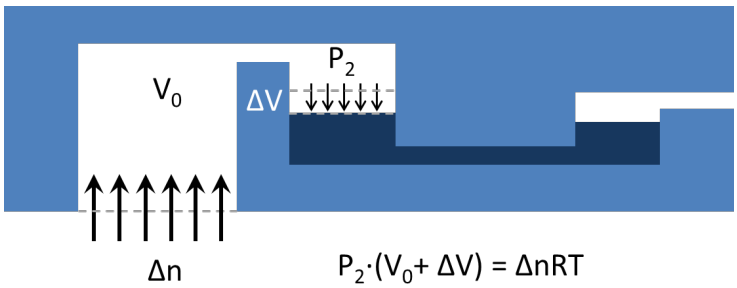 System stabilizes to P_2 while analysis chamber is filling.

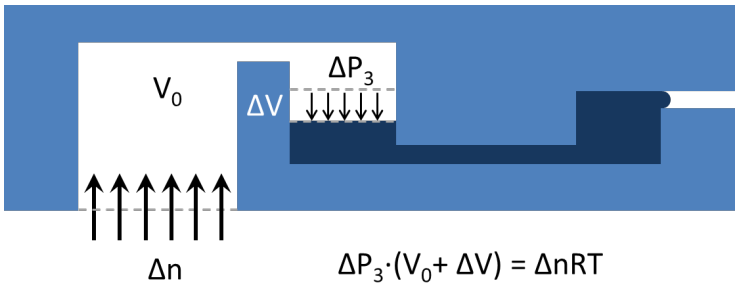

Once the analysis chamber is completely filled, a second pressure transient occurs: Again, the pressure first increases due to the change in cross-section between analysis chamber and the exit channel.

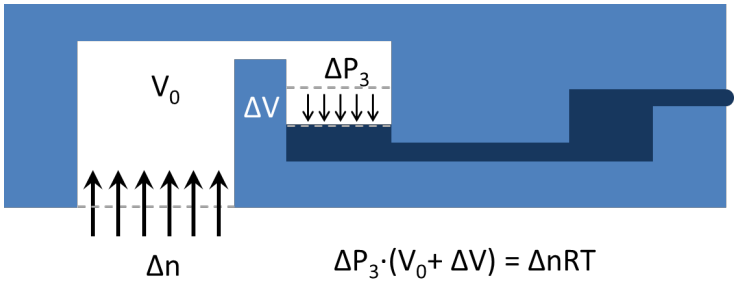

Afterwards, pressure drops once the sample gets the exit of the device.

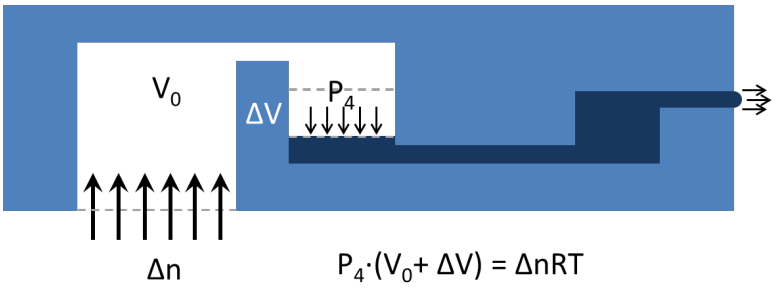

System stabilizes to P_4 until the sample chamber is completely empty.

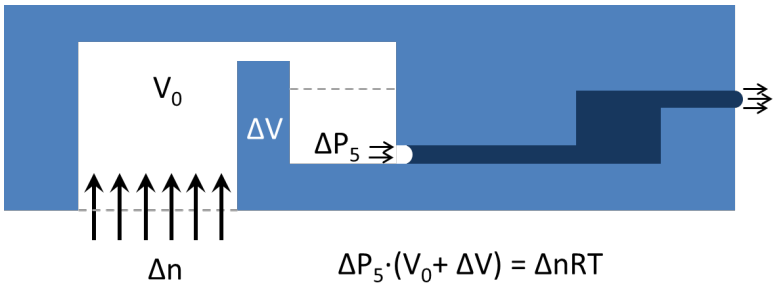

The force applied due to the CO_2 produced is the same, but now it is applied on a smaller area (onto the channel cross-section, instead of the sample chamber section). Thus, the pressure increases.

(iii) Analysis of the fluidic resistance

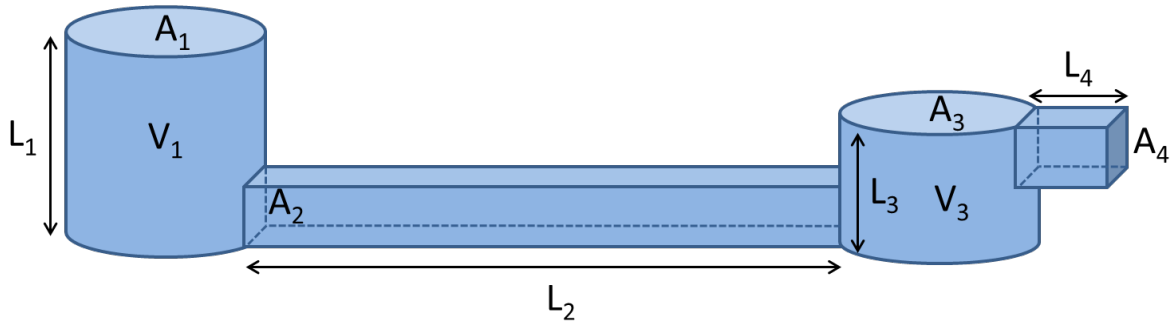

Schematic representation of the different components of the microfluidic device: V_1, sample volume (30 µL); A_1, sample chamber horizontal area ($\pi \cdot (2\ mm)^2 = 4 \cdot \pi\ mm^2$); L_1, sample chamber height (≈ 2 mm); A_2, interconnecting channel transversal area (0.02 mm^2); L_2 interconnecting channel length (13 mm); V_3, analysis chamber volume (15 µL); A_3, analysis chamber horizontal area ($\pi \cdot (2\ mm)^2 = 4 \cdot \pi\ mm^2$); L_3, analysis chamber height (≈ 1 mm); A_4 exit channel transversal area (0.02 mm^2); L_4, exit channel length (1 mm).

Variations in the pressure value at the CO_2/sample interface have been described above, and can be directly related with sample flow rate, according to the next expression:

$$\Delta P = \left(P_{interface\ CO_2/sample} - P_{atm}\right) = R_{total} \cdot Q$$

where:

$$R_{total} = R_1 + R_2 + R_3 + R_4 = k \cdot \left(\frac{L_1}{A_1} + \frac{L_2}{A_2} + \frac{L_3}{A_3} + \frac{L_4}{A_4}\right)$$

$$R_{total} = k \cdot (0.066\ mm^{-1} + 650\ mm^{-1} + 0.083\ mm^{-1} + 50\ mm^{-1})$$

Therefore, it can be concluded that in our design: $R_{total} \approx R_2$, thus, flow rate value (Q) in steady regions (Region 2 and Region 4 in Fig 4) is mainly controlled by the geometry of the connecting central microchannel.